

PAPER

Improvement of dielectric properties and energy storage performance in sandwich-structured P(VDF-CTFE) composites with low content of GO nanosheets

To cite this article: Lian Cheng *et al* 2021 *Nanotechnology* **32** 425702

View the [article online](#) for updates and enhancements.



ECS **240th ECS Meeting**
Digital Meeting, Oct 10-14, 2021

**Register early and save
up to 20% on registration costs**

Early registration deadline Sep 13

REGISTER NOW

Improvement of dielectric properties and energy storage performance in sandwich-structured P(VDF-CTFE) composites with low content of GO nanosheets

Lian Cheng^{1,2}, Kai Liu^{2,3}, Mengqi Wang³, Pengyuan Fan³,
Changrong Zhou⁴, Alexander N Vtyurin⁵, Heming Deng⁶, Ling Zhang⁷,
Haibo Zhang^{3,*}, Yongming Hu^{1,*}, Bo Nan^{2,3,*} and Yang Liu^{8,*}

¹ Hubei Key Laboratory of Ferro- & Piezoelectric Materials and Devices, Faculty of Physics and Electronic Science, Hubei University, Wuhan, 430062, People's Republic of China

² Guangdong HUST Industrial Technology Research Institute, Guangdong, 523808, People's Republic of China

³ School of Materials Science and Engineering, State Key Laboratory of Material Processing and Die & Mould Technology, Huazhong University of Science and Technology, Wuhan, 430074, People's Republic of China

⁴ College of Materials Science and Engineering, Guilin University of Electronic Technology, Guilin, 541004, People's Republic of China

⁵ Kirensky Institute of Physics SB RAS, Akademgorodok 50/38, Krasnoyarsk, 660036, Russia

⁶ State Grid Electric Power Research Institute Luoyu Road 143, Wuhan 430074, Hubei, People's Republic of China

⁷ School of Mechanical and Electrical Engineering, Shihezi University, Shihezi, People's Republic of China

⁸ School of Artificial Intelligence and Automation, Huazhong University of Science and Technology, Wuhan, 430074, People's Republic of China

E-mail: hbzhang@hust.edu.cn, huym@hubu.edu.cn, bonan@hust.edu.cn and yangliu30@hust.edu.cn

Received 10 May 2021, revised 27 June 2021

Accepted for publication 8 July 2021

Published 26 July 2021



CrossMark

Abstract

Polymer-based dielectric capacitors play a notable part in the practical application of energy storage devices. Graphene oxide (GO) nanosheets can improve the dielectric properties of polymer-based composites. However, the breakdown strength will greatly reduce with the increase of GO content. Hence, the construction of sandwich structure can enhance the breakdown strength without reducing the dielectric constant. Herein, single-layered and sandwich-structured poly(vinylidene fluoride-co-chlorotrifluoroethylene) (P(VDF-CTFE)) nanocomposites with low content of GO nanosheets (<1.0 wt%) are prepared via employing a straightforward casting method. Compared with the single-layered composites and pure P(VDF-CTFE), the sandwich-structured composites exhibit comprehensively better performance compared. The sandwich-structured composite with 0.4 wt% GO nanosheets show an excellent dielectric constant of 13.6 (at 1 kHz) and an outstanding discharged energy density of 8.25 J cm⁻³ at 3400 kV cm⁻¹. These results demonstrate that the growth of the dielectric properties is owing to 2D GO nanosheets and the enhancement of breakdown strength due to the sandwich structure. The results from finite element simulation provide theoretical support for the design of high energy density composites.

Supplementary material for this article is available [online](#)

* Authors to whom any correspondence should be addressed.

Keywords: polymer matrix composites, thin films, finite element analysis, sandwiched-structured

(Some figures may appear in colour only in the online journal)

1. Introduction

Despite dielectric capacitors with the high power density and the ability to charge and discharged rapidly, the traditional dielectric capacitor with a low energy storage density. Conventional dielectric capacitors are bulky and are used to increase the energy storage density for a variety of practical applications, such as defense, industrial lasers, medical equipment and advanced pulsed power systems. Thus, the trend that developing advanced dielectric capacitors with both high energy storage density and lightweight is more and more obvious. In order to tackle the above problems, a host of research efforts have been made to study and prepare polymer-based nanocomposites, which reconcile the advantages of nanofillers and polymers, acquiring favorable energy storage performance [1–4]. The charged and discharged process is closely bounded with the polarization and depolarization of dielectric capacitors [5]. Meanwhile, energy loss is inevitable in the process of charging and discharging, and the relevant energy density can be computed by following formulas:

$$U = \int_0^{D_{\max}} EdD, \quad (1)$$

$$U_e = \int_{P_r}^{D_{\max}} EdD, \quad (2)$$

where U is the energy density, U_e is the discharged energy density, P_r is abbreviated from remnant polarization. D presents the electric displacement and E is the applied electrical field, respectively. Accordingly, D is related to the applied electric field and can be written as

$$D = \varepsilon_0 \varepsilon_r E, \quad (3)$$

$$D = \varepsilon_0 E + P, \quad (4)$$

where ε_0 and ε_r represent the vacuum permittivity and the relative permittivity of materials. P represents the polarization, based on equation (4), which is positively correlated with D . Combining the above formulas, it is revealed that the breakdown strength (E_b) and the maximum electric displacement (D_{\max}) are pivotal value to enhance the discharged energy density (U_e) of dielectric capacitors [6, 7].

Compared with ceramic-based dielectrics, polymer-based dielectric materials are lightweight and easy to process and exhibit incomparable mechanical and functional properties such as high flexibility and electrical breakdown strength [8–11]. In fact, due to the low dielectric constant values (about 2–10) and energy storage density (around 1–3 J cm⁻³), most polymers are unsuitable for dielectric material applications unless being constructed into a composite structure, as combining the fillers with the polymer can endow the composite with both advantages, i.e. high dielectric permittivity from fillers and flexibility from the polymers. Therefore, some researchers have introduced ceramic nanoparticles, for

instance, SrTiO₃, BaTiO₃ into polymers [2, 12–18]. With the continuous addition of ceramic nanoparticles, the energy storage performance of polymer matrix composites will be distinctly enhanced. Nevertheless, the energy storage density of the composites decreases with the excessive addition of ceramic nanoparticles, which is in virtue of: (1) on account of the poor compatibility of the filler and the surface energy difference between the ceramic nanoparticles and the polymer matrix, there will be interface mismatch phenomenon. (2) Since the poor dispersion of fillers, the addition of excessive ceramic nanoparticles will make the nanoparticles overlap, easily forming conductive paths and weakening the breakdown field strength of composites [19–23]. In contrast with the zero-dimensional fillers (generally over 40 vol%), fewer one-dimensional (1D) and two-dimensional (2D) nanomaterials (generally less 10 vol%) (e.g carbon nanotubes and graphene oxide (GO) nanosheets) with large aspect ratios could improve the energy storage performance [13, 24–29]. Moreover, the lower specific surface of the 2D GO nanosheets are lower than 0D and 1D fillers, which can weaken surface energy and improve the compatibility with polymer matrix, and then improve the energy storage density [30–32]. The 2D GO nanosheets are dispersed in the polymer matrix, which has great effects on blocking the charge migration, making the breakdown path edge more zigzags, thus improving the internal E_b of the composites, and further improving the U_e of the composite material. Therefore, as a good choice of nanofillers, 2D nanosheets are expected to obtain excellent energy performance under the condition of low loading of nanofillers.

Apart from adding fillers with high dielectric constant to the polymer matrix, changing composite structures is also an effective strategy for promoting energy storage performance. Composite with sandwich structure has attracted much attention owing to the ability to improve the dielectric constant and high breakdown strength [8, 16, 33–49]. For instance, the ‘hard layer’ (high E_b) of sandwich-structured composite embeds into two ‘soft layers’ with high dielectric constants [14]. Such a design considerably increases the energy density, on account of the high polarization induced by the interface between ‘soft layers’ and ‘hard layer’ and the high breakdown strength generated by electric field regulation between dielectric layers.

Since GO nanosheets have an extremely high dielectric constant (~10 000 under 100 Hz), it is an optimal candidate to be a filler for preparing a composite and a commonly used additive in many different fields. Additionally, GO is a graphene derivative, which has a lot of oxygen-containing functional groups on its surface, which is helpful for GO to be compatible with the poly(vinylidene fluoride-co-chlorotrifluoroethylene) (P(VDF-CTFE)) matrix when mixing, constituting a uniform distribution of GO nanosheets in the P(VDF-CTFE) matrix. Therefore, in this report, GO nanosheets are synthesized by the Hummer method and later

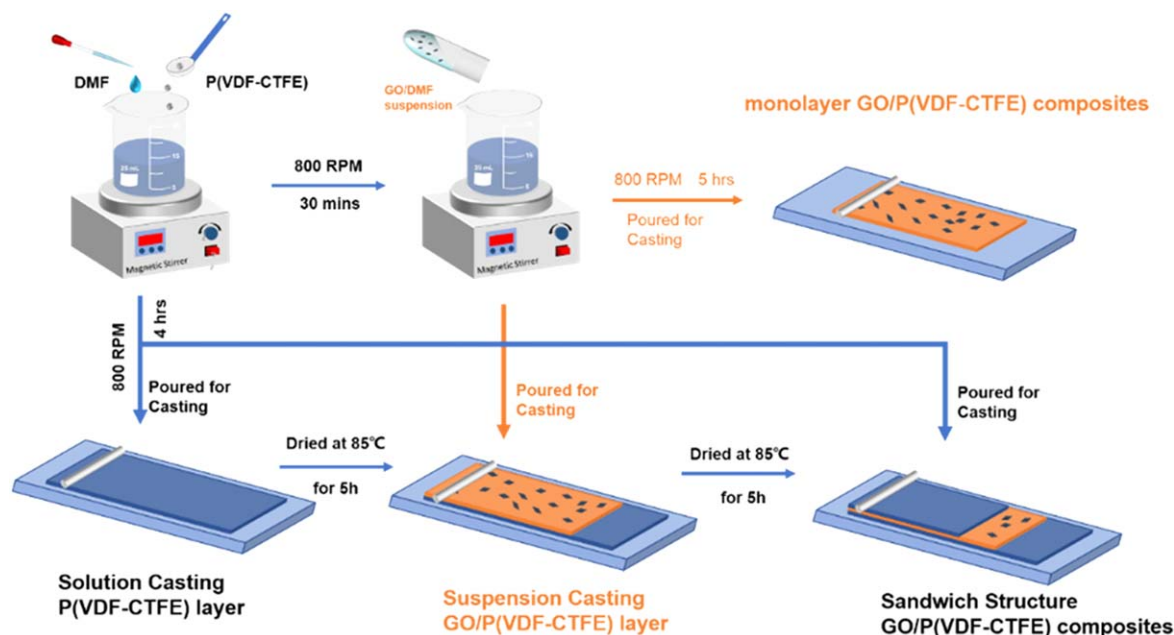


Figure 1. Schematic picture of processing both single-layered and sandwich-structured GO/P(VDF-CTFE) composites.

incorporated into P(VDF-CTFE) polymer to prepare both single-layered and sandwich-structured GO/P(VDF-CTFE) nanocomposites [23, 33]. The results show that the introduction of 2D GO nanosheets and the construction of sandwich structure are helpful to promote the dielectric and energy storage performance, providing a new idea of manufacturing energy storage device in the viewpoint of optimizing the composition and structure of the materials.

2. Experimental

2.1. Synthesis of GO nanosheets

GO nanosheets were synthesized via a modified Hummer's method, as shown in figure S1 (available online at stacks.iop.org/NANO/32/425702/mmedia) [50]. 1.0 g graphite (Macklin, >99.9%) and 0.5 g NaNO_3 (Aladdin, >99.0%) were added in 23 ml of H_2SO_4 (Macklin, >98.0%) and stirred slowly in an ice bath for 5 min, followed by adding 3.0 g KMnO_4 (Aladdin, >99.0%) into the as-prepared mixture. After stirring for 2 h in an ice bath, the temperature was gradually ascended to 35 °C then the mixture was continued stirring at 800 rpm for 40 min. Consequently, 45 ml deionized water was added to the suspension and the temperature increased to 98 °C and stirred for 30 min. Ultimately, 150 ml deionized water together with 10 ml H_2O_2 (Aladdin, >30.0%) was added to complete the reaction. The resulting suspension was centrifuged at 7200 rpm then washed several times via deionized water, afterwards dried in the oven at 100 °C for 12 h. Subsequently, 0.2 g obtained graphite oxide was dispensed into four 50 ml centrifuge tubes and sonicated for 1 h. After that, the centrifuge tubes were centrifuged at 9000 rpm for 10 min, and the GO nanosheets were stoved at 60 °C for 12 h in the oven for further use.

2.2. Fabrication of the single-layered and sandwich-structured GO/P(VDF-CTFE) composites

Figure 1 shows the schematic picture of preparing single-layered and sandwich-structured GO/P(VDF-CTFE) composites. Poly(vinylidene fluoride-co-chlorotrifluoroethylene) (P(VDF-CTFE), Solef 31508, Solvay) was firstly dissolved in N,N-dimethylformamide (DMF, Aladdin, >99.9%) then stirred at 800 rpm for 30 min, to obtain the P(VDF-CTFE)-DMF solution. Then, GO-DMF suspension was homogenized by using an ultrasonic cell crusher (JY92-IIN, SCIENTZ). The GO-DMF suspension was slowly poured into the P(VDF-CTFE)-DMF solution in the mass (1:12) and stirred for 5 h to obtain a series of the well-dispersed $x\text{GO-P(VDF-CTFE)}$ ($x = 0.2, 0.4, 0.6$ and 0.8 wt%). The mixed suspension was scraped manually via a glass rod on 10×10 cm² quartz glass plates. The green composites were stoved at 85 °C for 5 h in a vacuum drying chamber, followed by heating them in the oven at 205 °C for 10 min. The as-heated films were then quickly quenched in the ice water.

There are several different types of that the sandwich-structured GO/P(VDF-CTFE) composites, which contain various amounts of GO nanosheets in P(VDF-CTFE), were abbreviated as $0-x-0$ GO/P(VDF-CTFE) composite, where $x = 0.2, 0.4, 0.6$ and 0.8 wt%. Similar to the above-mentioned preparing process of the single-layered composite, the sandwich-structured samples were processed in a layer-by-layer fashion by casting. The first pure P(VDF-CTFE) layer was scrapped on a glass substrate. The second layer composed of GO/P(VDF-CTFE) was directly covered on the previous P(VDF-CTFE) film, while the last layer of pure P(VDF-CTFE) was repeatedly cast on top of the second layer. Before casting each layer, the previous layer was heated at 85 °C for 5 h, to assure a non-collapsed sandwich-structured. Consequently, the sandwich-structured samples can be easily stripped from the glass substrate, and all of the composite samples were

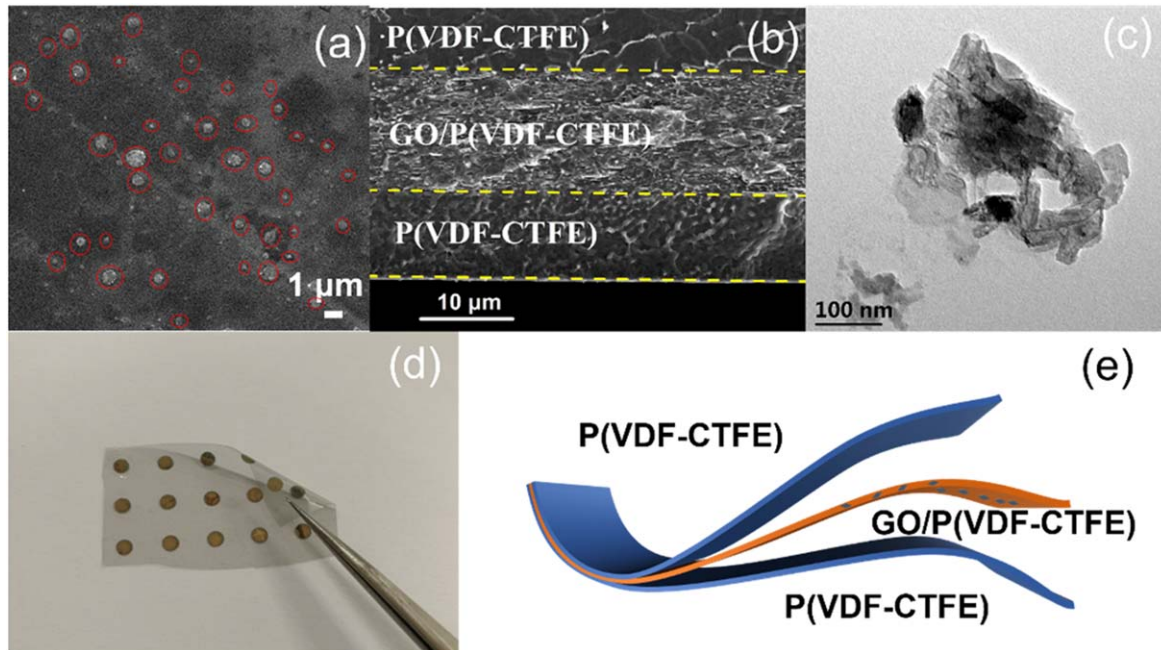


Figure 2. (a) SEM image of single-layered 0.4 wt% GO/P(VDF-CTFE) film. Graphene oxide particles are labeled by red circles. (b) Cross-section SEM image of 0-4-0 GO/P(VDF-CTFE) composites. (c) TEM image of GO nanosheets. (d) Optical images of the 0-4-0 GO/P(VDF-CTFE) composite film. (e) Schematic structure of the sandwich-structured GO/P(VDF-CTFE) composites.

transferred into an oven and kept at the temperature of 205 °C for 10 min, then quickly quenching.

2.3. Characterization

The cross-sectional diagrammatic form of the composite structure was pictured by scanning electron microscopy (SEM, Quanta 250FEG, FEI, Ltd). GO nanosheets were observed by a transmission electron microscopy (TEM, 2100, JEOL, Ltd). Before analyzing electric behaviors, two layers of gold (a thickness of ~57 nm for each layer) were sputtered on two sides of the composites via an ion sputter coater (ISC, SBC-12, KYKY Tech. Co., Beijing, China) by a metal mask with uniformly dispersed eyelets (an area of ~4.9 mm²). The polarization–electrical field (P – E) hysteresis loops of the composites were measured at 100 Hz by a Precision Multiferroic Materials Analyzer (Radiant Inc. US). The E_b of composites can be achieved from the P – E hysteresis loops under applied electric fields when breakdown occurred. The dielectric constant and the dielectric loss of the sandwich-structured composites were measured using a precision LCR meter at room temperature (TH2827C, Tonghui Electronic Co. Ltd, Jiangsu, China) by scanning each sample within a range of frequency from 100 Hz to 1 MHz. The finite element simulation of electric field distribution was performed for the single-layered composites and sandwich-structured composites with a dimension of $9.3 \times 3.1 \mu\text{m}^2$ using ANSYS Maxwell 16.0 software.

3. Results and discussion

The SEM image describes that the GO nanosheets are uniformly dispersed in P(VDF-CTFE) (figure 2(a)). White dots

marked with red circles are GO nanosheets, and the large black area is P(VDF-CTFE). Obviously, the GO nanosheets are closely bound to the P(VDF-CTFE) matrix. It is detected that no defects such as holes and cracks on the surface of the single-layered GO/P(VDF-CTFE) composites, indicating excellent compatibility (figure 2(a)), because the oxygen-containing groups of GO nanosheets and the P(VDF-CTFE) matrix can form a close binding force between the interface. From its cross-section image in figure 2(b), the 0-4-0 GO/P(VDF-CTFE) composite is in the form of a sandwich structure, consistent with experimental design and the picture drawn in figure 2(e). It can be observed that the interface between the layers is dense and uniform, and there is no obvious void and crack. The clear boundary between the inner layers indicates that layers are not fused with each other. When measuring the total thickness of sandwich-structured composite, which is approximately 25 μm . While the TEM image (figure 2(c)) verifies the size of GO nanosheets is in the nanoscale. It also confirms that GO nanosheets has multiple layers. The macrostructure of GO nanosheets is shown in figure S3. The photograph in figure 2(d) shows good flexibility with the transparency of the 0-4-0 composite, where similar properties can be found in the other sandwich-structured composites.

The dielectric properties for sandwich-structured GO/P(VDF-CTFE) composites with numerous contents of GO nanosheets were studied by a broadband dielectric spectroscopy at room temperature in figure 3. With a rise in filler content, the dielectric constants of the sandwich-structured GO/P(VDF-CTFE) composites all increase uniformly compared to the pure P(VDF-CTFE) in the low range frequency (under 10⁵ Hz). The increase in the value of dielectric constant with increasing GO nanosheets content in the

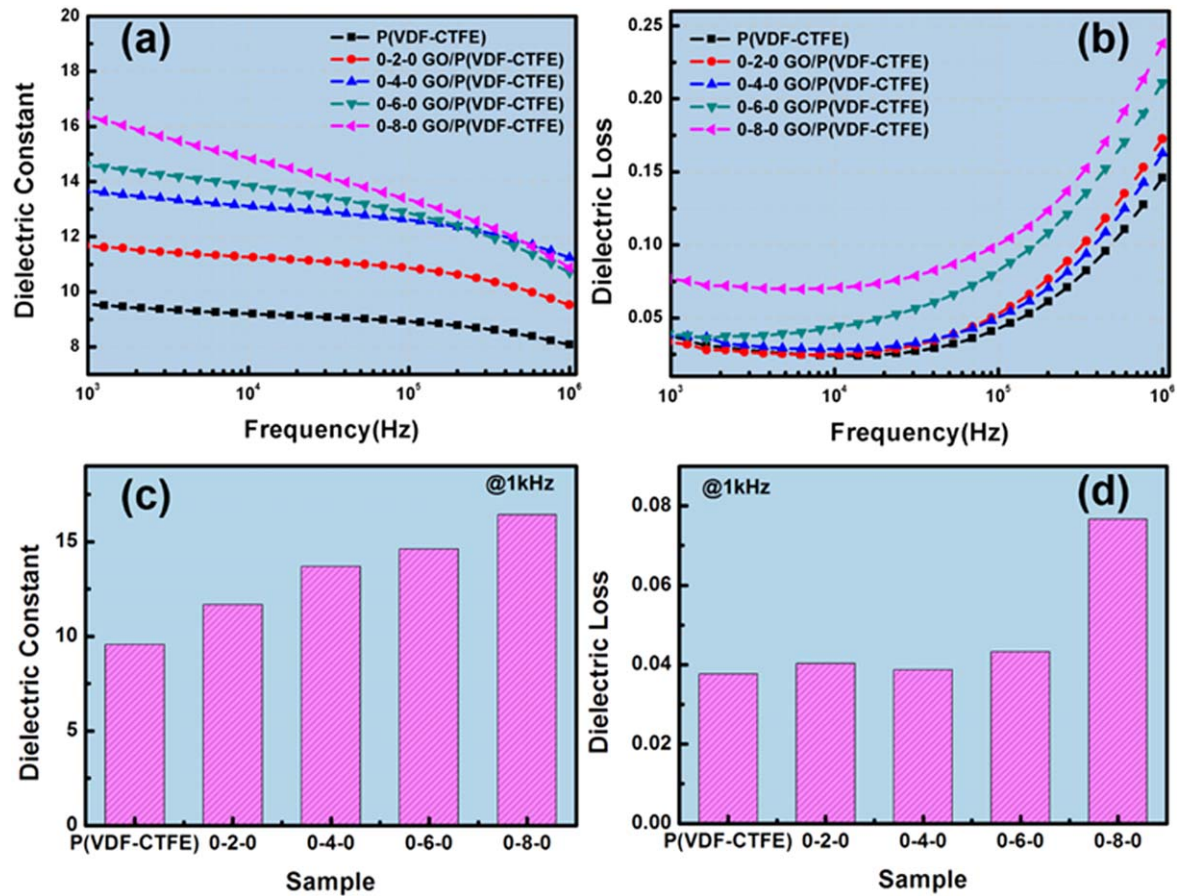


Figure 3. (a) Dielectric constant and (b) dielectric loss of pure P(VDF-CTFE) the several sandwich-structured composites under different frequencies. (c) Dielectric constant and (d) dielectric loss of pure P(VDF-CTFE) the various sandwich-structured composites at 1 kHz.

composites can be explained by two factors: (i) introduction of high dielectric constant GO nanosheets and (ii) accumulation of a large amount of charges at the interfaces between the fillers and the matrix. When GO nanosheets concentration increases, the quantity of interfacial charges increases, and as a result, an enhancement of the interfacial polarization density and dielectric constant is observed. The dielectric constants of all sandwich-structured GO/P(VDF-CTFE) composites decrease slightly with increasing frequency in figure 3(a). However, the dielectric constants sharply decrease above a frequency of 10^5 Hz, particularly for the composites with 0.8 wt% GO nanosheets. This can be interpreted when the frequency of the exterior electric field surpasses the frequency of dielectric relaxation, the mobility of polar groups is not enough to affect the dielectric constant, which is a common phenomenon of dielectric relaxation [20]. It's worth noting that the dielectric constant of sandwich-structured composites is over 10, which is higher than that of the pure P(VDF-CTFE) film (~ 9.5). While the frequency is below 10^5 Hz, the dielectric losses of the composites exhibit low values under less than 0.08 (figure 3(b)). Additionally, it can be observed that GO nanosheet composites have higher dielectric loss than pure P(VDF-CTFE) films due to the interfacial polarization, which results from the large contrast between the dielectric constant and conductivity of the filler and the matrix. It is notable that the 0-8-0 GO/P(VDF-CTFE) composites exhibit greater dielectric loss. For the composites, the main reason for

the dielectric loss is the orientation polarization of polarization units and space charges. The additional GO nanosheets create more interfacial area which, in turn, can generate more space charges and additional polarization units. Also, the electric field formation with GO nanosheets embedded in a continuous P(VDF-CTFE) matrix depends on the polarization of inorganic particles and the distance between them. As the filler amounts increase, the distance between the fillers will get closer and closer, leading to the rapid formation of electric field to cause thermal dielectric loss. All the composites show a sharp increase from 10^4 to 10^6 Hz (figure 3(b)). It is typical glass transition relaxation of P(VDF-CTFE). The dielectric constant and the dielectric loss of pure P(VDF-CTFE) and all sandwich-structured GO/P(VDF-CTFE) composites are displayed at 10^3 Hz in figures 3(c) and (d). Comparing 0-4-0 sandwich-structured GO/P(VDF-CTFE) composite with other composites, the dielectric constant is relatively high and the dielectric loss is lower, which are important reasons to choose it for the optimal composite.

The dielectric constant is one important parameter in improving energy storage density. Aims to study the energy storage performance of the composites, the E_b value of dielectric materials is calculated from a two-parameter Weibull distribution, which is denoted by the consequent equations:

$$X_i = \ln(E_i), \quad (5)$$

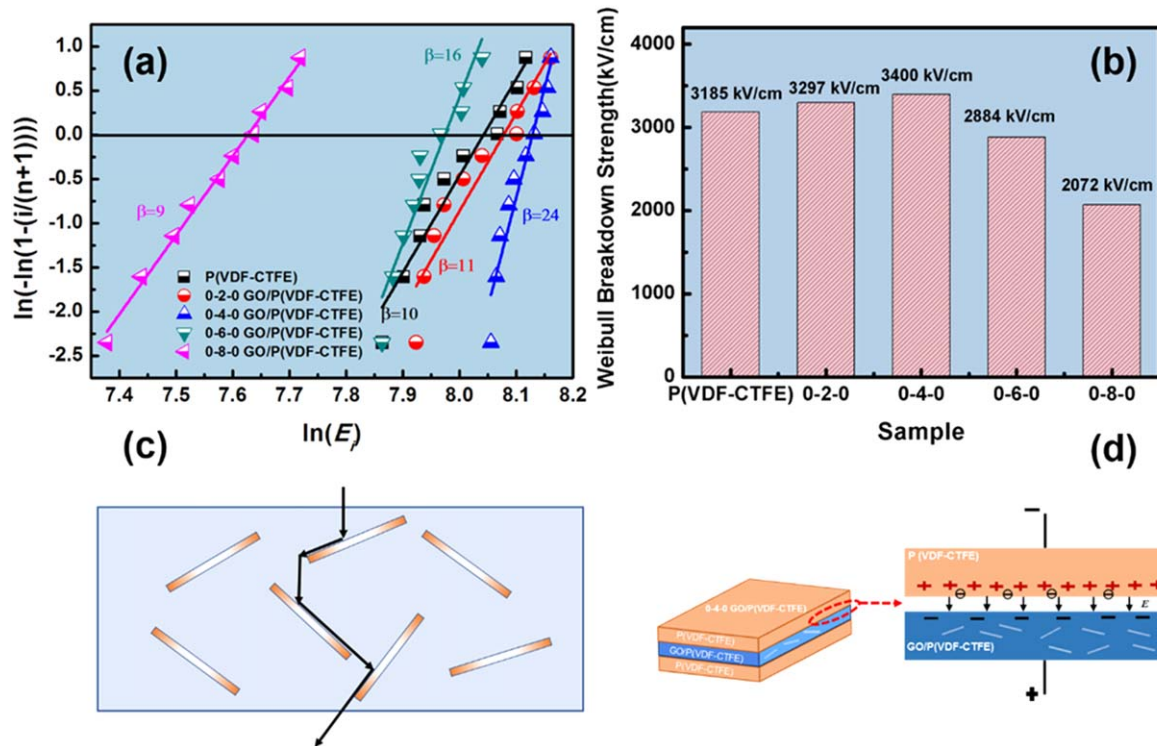


Figure 4. (a) Weibull distribution and (b) Weibull breakdown strength of the pure P(VDF-CTFE) the different sandwich-structured composites. (c) Schematic diagram of the breakdown path in composites. (d) Schematic diagram of interface hindrance effect of sandwich-structured composites.

$$Y_i = \ln\left(-\ln\left(1 - \frac{i}{n}\right)\right). \tag{6}$$

The n samples are sorted from smallest to largest in the order of breakdown strength values (this work the $n = 10$) and the breakdown strength of sample i is given as E_i . X_i and Y_i are the vertical and horizontal coordinates of the point i of the Weibull distribution, and the relationship between X and Y should be linear. The shape parameter (β), equivalent to the slope of the line, indicates how reliable the data is, as higher β means better reliability. Weibull's distribution is achieved via presenting equations (5) and (6) and linearly fitted (figure 4(a)). All sandwich-structured GO/P(VDF-CTFE) composites own high β values, however, the 0-4-0 GO/PVDF-CTFE composite has the highest β value, indicating the stability of the data in this specific composition, which is advantageous for practical applications (figure 4(b)). Therefore, the average E_b of all sandwich-structured composites are determined by the points where the bottom axis across $Y_i = 0$ touched the linear lines. The pure P(VDF-CTFE) film and 0-2-0, 0-4-0, 0-6-0, 0-8-0 composites showed the average E_b of 3185, 3279, 3400, 2884 and 2072 kV cm^{-1} , respectively (figure 4(b)). With the increasing GO nanosheets content, E_b will increase first and then decrease, reaching maximum value when the filling amount is 0.4 wt%. It is noting that with 0.4 wt% of GO nanosheets, the E_b reaches 3400 kV cm^{-1} , which is an improvement of $\approx 106\%$ than the pure P(VDF-CTFE) film, attributed to lots of electrons moving towards GO nanosheets, some scattered by phonons or imperfections, and others blocked to form some tortuous breakdown path for

increasing E_b (figure 4(c)). However, when the content of GO is larger than 0.4 wt%, the E_b of sandwich-structured composites begins decreasing. The E_b decreases with more GO nanosheets contributes to three aspects: (1) the increasing content of GO nanosheets shorten the distance between GO nanosheets, and some may contact directly. It is easy to form the conductive path under applied electric field, which can reduce the E_b of composites; (2) because GO nanosheets are conductive, excessive GO nanosheets will increase the probability of electric field breakdown in the polymer-based composites; (3) the aggregation of fillers for cracks, pores, and voids, which is also could decrease the E_b of composites [23]. The E_b single-layered composites are less than 3000 kV cm^{-1} , as observed in figure S4. Obviously, the E_b of sandwich-structured composites are higher than single-layered composites, which attributed to two factors: (1) when act the insulating P(VDF-CTFE) layers the external layers of the sandwich-structured composites, the breakdown path will be suppressed. (2) The sandwich-structured composites exist the interfacial hindrance effects. The interfacial hindrance effect of sandwich-structured between the outer and inner layers due to the difference in dielectric constants, as observed in figure 4(d). When the applied electric field is increasing, positive charges will gather underneath the outer layer, so that negative charges will appear at the upper part of the inner layer. Then, an internal electric field will be formed between the interfaces, and the internal electric field and the applied electric field in opposite directions, which will hinder the charge migration and thus inhibit the formation of electric breakdown. The interfacial hindrance effect exists in the

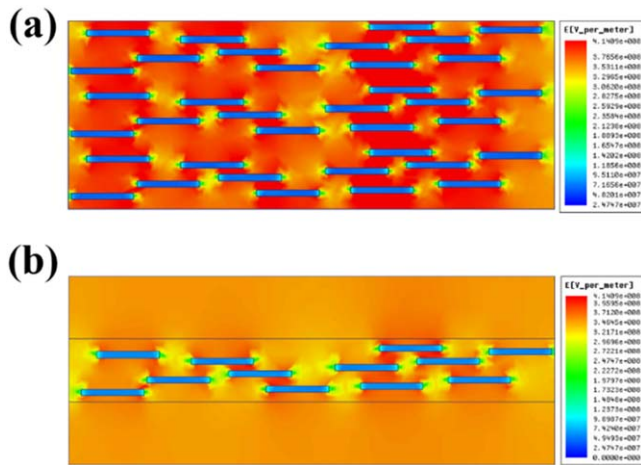


Figure 5. Finite element simulation of (a) single-layered composites and (b) sandwich-structured composites.

sandwich-structured composites, which will enhance the E_b and thus enhance its energy storage performance [47, 51].

In order to further visually comprehend the electric field distribution of the single-layered and sandwich-structured composites, which were directly mirrored via finite element simulation as manifested in figure 5. The color scale bars imply the strength of the local electric field strength, the higher the electrical field strength is, the darker the color is, and vice versa. No matter it is a single-layered composite or a sandwich-structured composite, low and distortion electric field strengths are clearly visible in the surrounding area of GO nanosheets, which stems from the difference in permittivity between the P(VDF-CTFE) matrix and the GO nanosheets. There are local electric field distortion regions between adjacent filling areas in single-layered composites, which may come from electric field paths thus causing many potential breakdown regions and reducing the E_b (figure 5(a)). But for the sandwich-structured composite, it is clearly seen that the electrical field distribution of films is more uniform due to the lighter color depicted in figure 5(b). The low dielectric constant P(VDF-CTFE) layer is introduced into the outer position of the sandwich-structured composite, which can inhibit breakdown paths of the material, because of redistribution of the electric field. Since a higher electric field is induced in the outer layer of the sandwich-structured composite, the electric field intensity in the inner layer gets reduced. Therefore, the sandwich-structured composites show an overwhelming higher value of E_b than the single-layered composites.

The polarization–electrical field (P – E) hysteresis loops of single-layered and sandwich-structured GO/P(VDF-CTFE) composites with many filling amounts were measured under different fields (figures S5 and 6(a)). Figure S6 represents P – E loops of all sandwich-structured GO/P(VDF-CTFE) under various electric fields. The discharged energy density increases with an increasing GO content at the same applied electric field (figure 6(b)), indicating that the addition of the high dielectric constant of GO nanosheet can promote the polarization, thereby improving the energy density. The

discharged efficiency (η) of the dielectric materials is computed by the following equation:

$$\eta = \frac{\text{discharged energy density}}{\text{charged energy density}}. \quad (7)$$

The η value of sandwich-structured composites declines with the climb of electric field, due to the increase of conductive loss caused by the high electric field (figure 6(c)). It is noteworthy that the sandwich-structured composites with low-level 0.4 wt% possess the highest U_e of 8.25 J cm^{-3} , which is 42% higher than the highest U_e of 5.8 J cm^{-3} of the pure P(VDF-CTFE) film. The U_e of sandwich-structured composites with the amount of GO higher than 0.4 wt% show much lower energy density owing to the possible increased defects beyond the optimal filler contents. (figure 6(d)). The discharged efficiencies of all sandwich-structured samples were displayed showing a decreasing trend of efficiency with an increasing GO content. For the single-layered composites, the discharged energy density and discharged efficiency are depicted in figure S7. In addition, the discharged energy densities of single-layered are much lower than those on sandwich-structured composites, because of the higher E_b of sandwich-structured composites. In comparison with the single-layered composite, the 0-4-0 GO/P(VDF-CTFE) composites show the largest enhancement in energy storage performance. Therefore, the 0-4-0 GO/P(VDF-CTFE) is the optimal composition among all the sandwich-structured composites.

The schematic diagram of increasing the energy density of GO/P(VDF-CTFE) composites is depicted in figure 7(a). In order to further prove figures 7(a) and (b) is illustrated by the discharged energy density of the two structures under different electric fields. As shown in figure 7(b), The comparison in energy storage performance between sandwich-structured composite and single layer composite with 0.4 wt% GO loading clearly demonstrates an enhancement of 248.2% in discharged energy density (8.25 J cm^{-3} compared to 2.37 J cm^{-3} for GO/P(VDF-CTFE) single layer film) mainly dependent on the higher breakdown strength, showing the superiority of sandwich structure in achieving high energy storage density. In the sandwich-structured composites, the outer layer is pure P(VDF-CTFE) without the presence of GO nanosheets, which gives rise to weaker charge injection. Moreover, in the sandwich-structured composites, the dielectric mismatch at the macroscopic interfaces between adjacent layers enables creating energy barrier for the charge migration inside the composite films. This explains that the sandwich structure can increase the breakdown field to improve the discharged energy density. Together with the addition of 0.4 wt% GO, the sandwich-structured composites can achieve remarkable discharged energy density and higher efficiency due to their optimal composition and structure. Comparison of weight content, dielectric constant (at 10^3 Hz) and discharged energy density in this work and other nanocomposites reported in the previous work presented in figure 8 [14, 52–56] and the detailed data are concluded in table 1. For example, BST-P(VDF-CTFE) and PPFPA@BST-P(VDF-CTFE) both with the filling content of 8 wt% exhibit

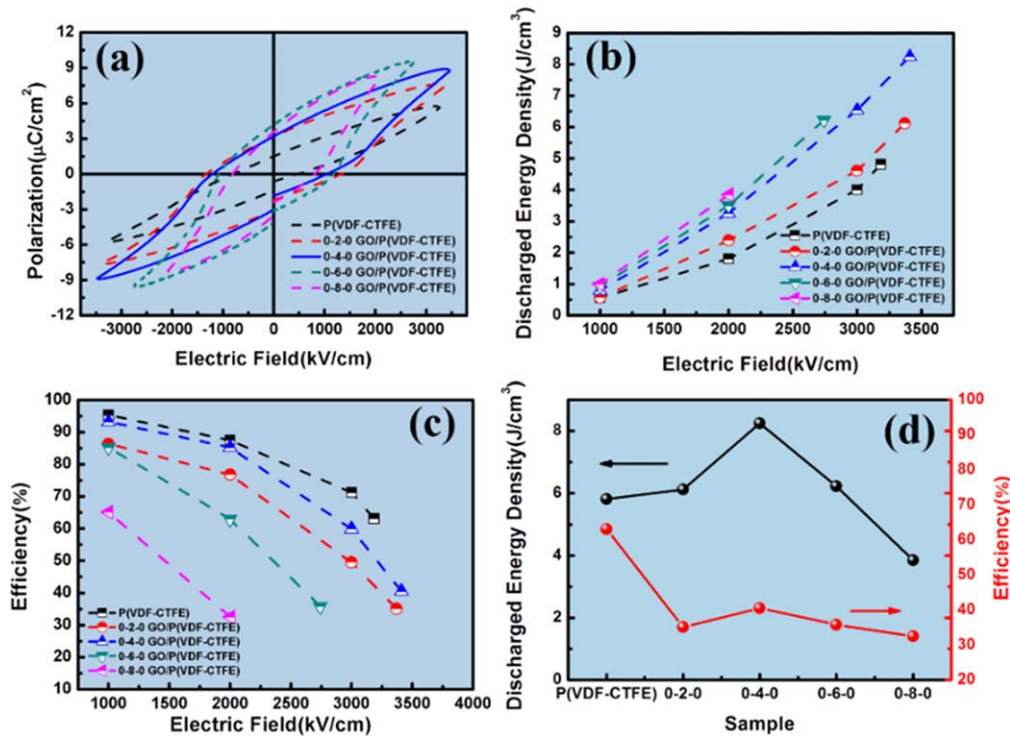


Figure 6. (a) $P-E$ loops, (b) discharged energy density, (c) efficiency, (d) discharged energy density, and discharged efficiency of the pure P(VDF-CTFE) and sandwich-structured composites.

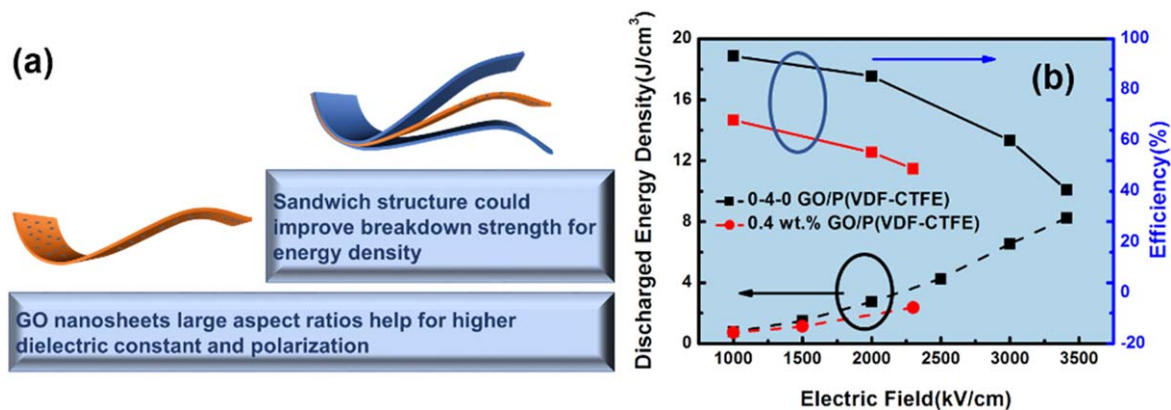


Figure 7. (a) Schematic diagram of the strategy for improving the energy density of GO/P(VDF-CTFE) composite. (b) The discharged energy density and efficiency of the single-layered 0.4 wt% composites and the sandwich-structured 0-4-0 composites.

the discharged energy density of 1.9 and 2.0 J/cm^3 along with dielectric constant of 10.5 and 10.2, respectively [54]. Their breakdown strengths are all less than 2600 kV/cm^{-1} , which is much lower compared to our work, further demonstrating the advantage of the sandwich structure than a single layer one. Meanwhile, the breakdown strength of sandwich-structured CNT(10 wt%)/PI is only 970 kV/cm^{-1} which leads the discharged energy density of that only 1.31 J/cm^3 [25]. In contrast, the breakdown strength of our work is 3.5 times higher than that of CNT/PI nanocomposites, because the breakdown strength of P(VDF-CTFE) is higher than that of PI [25]. As a result, the discharged energy density of our work is higher than that of CNT/PI nanocomposites.

4. Conclusions

The addition of 2D GO nanosheets to P(VDF-CTFE) matrix and the construction of sandwich structure can enhance the energy storage performance of the dielectric materials. As a result, the 0-4-0 sandwich-structured composite exhibits superior dielectric constant (13.6 at 1 kHz) and excellent discharged energy density (8.25 J/cm^3 at 3400 kV/cm^{-1}). The introduction of GO nanosheets improve dielectric constant and prevent electrons to form tortuous breakdown paths for increasing breakdown strength. The P(VDF-CTFE), as the outer layer in the sandwich structure, can prevent the conductive channel of the inner layer from extending to the outer

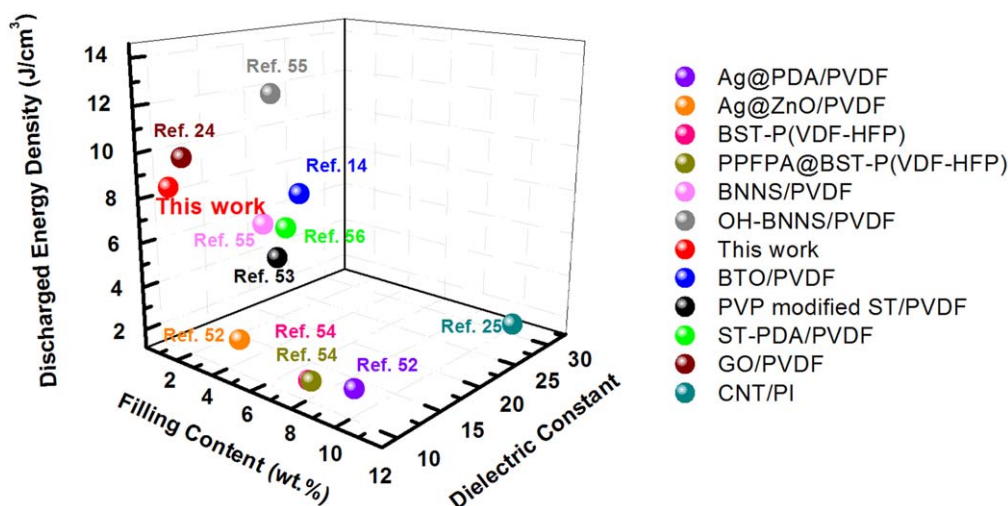


Figure 8. Comparison of weight content, dielectric constant and discharged energy density in this work and the nanocomposites reported in the previous work.

Table 1. Comparison of dielectric constant and discharged energy density of dielectric nanocomposites.

Dielectric nanocomposites	Filling content (wt%)	Dielectric constant (1 kHz)	Discharged energy density(J cm^{-3})	References
Ag@PDA/PVDF	10	10.4	2.33	[52]
Ag@ZnO/PVDF	5	9.4	2.9	[52]
BST-P(VDF-HFP)	8	10.5	1.9	[54]
PPFPA@BST-P(VDF-HFP)	8	10.2	2.0	[54]
PVDF/BNNS	6	10.2	8.0	[55]
PVDF/OH-BNNS	6	11.1	13.1	[55]
GO/P(VDF-CTFE)	0.4	13.6	8.25	This work
BTO/PVDF	8	9.5	9.72	[14]
PVP modified ST/PVDF	6.7	10	6.8	[53]
ST-PDA/PVDF	6.7	10.9	7.9	[56]
GO/P(VDF-HFP)	2	9.8	10	[24]
CNT/PI	10	31.3	1.31	[25]

layers under a high electrical field, thus improving the breakdown strength of the composite material. Finite element simulation proves the superiority of the introduction of 2D GO nanosheets and the stable properties of sandwich-structured composites. In summary, the construction of sandwich-structured composite film and the introduction of high dielectric constant fillers are effective strategies to further improve the energy storage performance in dielectric materials.

Acknowledgments

The authors gratefully acknowledge the support by the National Natural Science Foundation of China: 51902111; DongGuan Innovation Research Team Program: 2020607101007; Dongguan Postgraduate Joint Training (Practice) Workstation: 2019707102018; Guangdong HUST Industrial Technology Research Institute, Guangdong Provincial Key Laboratory of Manufacturing Equipment Digitization: 2020B1212060014.

Data availability statement

All data that support the findings of this study are included within the article (and any supplementary files).

ORCID iDs

Haibo Zhang <https://orcid.org/0000-0002-5544-531X>

Bo Nan <https://orcid.org/0000-0002-6580-7273>

References

- [1] Chen J, Daniels J E, Jian J, Cheng Z, Cheng J, Wang J, Gu Q and Zhang S 2020 Origin of large electric-field-induced strain in pseudo-cubic BiFeO_3 - BaTiO_3 ceramics *Acta Mater.* **197** 1–9
- [2] Jiang Y, Zhang X, Shen Z, Li X, Yan J, Li B W and Nan C W 2019 Ultrahigh breakdown strength and improved energy density of polymer nanocomposites with gradient distribution of ceramic nanoparticles *Adv. Funct. Mater.* **30** 1906112

- [3] Niu Y and Wang H 2019 Dielectric nanomaterials for power energy storage: surface modification and characterization *ACS Appl. Nano Mater.* **2** 627–42
- [4] Zhong S-L, Dang Z-M, Zhou W-Y and Cai H-W 2018 Past and future on nanodielectrics *IET Nanodielectr.* **1** 41–7
- [5] Lu X, Zhang L, Tong Y and Cheng Z Y 2019 BST-P(VDF-CTFE) nanocomposite films with high dielectric constant, low dielectric loss, and high energy-storage density *Composites B* **168** 34–43
- [6] Palneedi H, Peddigari M, Hwang G-T, Jeong D-Y and Ryu J 2018 High-performance dielectric ceramic films for energy storage capacitors: progress and outlook *Adv. Funct. Mater.* **28** 1803665
- [7] Prateek T V K and Gupta R K 2016 Recent progress on ferroelectric polymer-based nanocomposites for high energy density capacitors: synthesis, dielectric properties, and future aspects *Chem. Rev.* **116** 4260–317
- [8] Li Z, Shen Z, Yang X, Zhu X, Zhou Y, Dong L, Xiong C and Wang Q 2021 Ultrahigh charge–discharge efficiency and enhanced energy density of the sandwiched polymer nanocomposites with poly(methyl methacrylate) layer *Compos. Sci. Technol.* **202** 108591
- [9] Liu F, Li Z, Wang Q and Xiong C 2018 High breakdown strength and low loss binary polymer blends of poly(vinylidene fluoride-trifluoroethylene-chlorofluoroethylene) and poly(methyl methacrylate) *Polym. Adv. Technol.* **29** 1271–7
- [10] Zhang D, Liu W, Guo R, Zhou K and Luo H 2018 High discharge energy density at low electric field using an aligned titanium dioxide/lead zirconate titanate nanowire array *Adv. Sci.* **5** 1700512
- [11] Zhu Y, Jiang P and Huang X 2019 Poly(vinylidene fluoride) terpolymer and poly(methyl methacrylate) composite films with superior energy storage performance for electrostatic capacitor application *Compos. Sci. Technol.* **179** 115–24
- [12] Bi K, Bi M, Hao Y, Luo W, Cai Z, Wang X and Huang Y 2018 Ultrafine core–shell BaTiO₃@SiO₂ structures for nanocomposite capacitors with high energy density *Nano Energy* **51** 513–23
- [13] Gong L, Chen S H, Zhan S P, Sun X D, Yin B, Liu Z Y, Yang M B and Yang Y 2019 An enhancement on the dielectric performance of poly(vinylidene fluoride)-based composite with graphene oxide–BaTiO₃ hybrid *Nanocomposites* **5** 61–6
- [14] Hu P, Shen Y, Guan Y, Zhang X, Lin Y, Zhang Q and Nan C-W 2014 Topological-structure modulated polymer nanocomposites exhibiting highly enhanced dielectric strength and energy density *Adv. Funct. Mater.* **24** 3172–8
- [15] Liu K et al 2020 Enhanced energy storage performance of nanocomposites filled with paraelectric ceramic nanoparticles by weakening the electric field distortion *Ceram. Int.* **46** 21149–55
- [16] Sun Q, Wang J, Zhang L, Mao P, Liu S, He L, Kang F and Xue R 2020 Achieving high energy density and discharge efficiency in multi-layered PVDF-PMMA nanocomposites composed of 0D BaTiO₃ and 1D NaNbO₃@SiO₂ *J. Mater. Chem. C* **8** 7211–20
- [17] Zhang X, Shen Y, Zhang Q, Gu L, Hu Y, Du J, Lin Y and Nan C W 2015 Ultrahigh energy density of polymer nanocomposites containing BaTiO₃@TiO₂ nanofibers by atomic-scale interface engineering *Adv. Mater.* **27** 819–24
- [18] Zhu Y, Yuan S, Lu C, Xie B, Fan P, Marwat M A, Ma W, Liu K, Liu H and Zhang H 2018 High discharged energy density of nanocomposites filled with double-layered core-shell nanoparticles by reducing space charge polarization *Ceram. Int.* **44** 19330–7
- [19] Chen J, Wang Y, Xu X, Yuan Q, Niu Y, Wang Q and Wang H 2019 Ultrahigh discharge efficiency and energy density achieved at low electric fields in sandwich-structured polymer films containing dielectric elastomers *J. Mater. Chem. A* **7** 3729–36
- [20] Guo R, Luo H, Yan M, Zhou X, Zhou K and Zhang D 2021 Significantly enhanced breakdown strength and energy density in sandwich-structured nanocomposites with low-level BaTiO₃ nanowires *Nano Energy* **79** 105412
- [21] Luo H, Ma C, Zhou X, Chen S and Zhang D 2017 Interfacial design in dielectric nanocomposite using liquid-crystalline polymers *Macromolecules* **50** 5132–7
- [22] Pan Z, Liu B, Zhai J, Yao L, Yang K and Shen B 2017 NaNbO₃ two-dimensional platelets induced highly energy storage density in trilayered architecture composites *Nano Energy* **40** 587–95
- [23] Wang Z, Wang X, Sun Z, Li Y, Li J and Shi Y 2019 Enhanced energy storage property of plate-like Na_{0.5}Bi_{4.5}Ti₄O₁₅/poly(vinylidene fluoride) composites through texture arrangement *Ceram. Int.* **45** 18356–62
- [24] Chen J, Li Y, Wang Y, Dong J, Xu X, Yuan Q, Niu Y, Wang Q and Wang H 2020 Significantly improved breakdown strength and energy density of tri-layered polymer nanocomposites with optimized graphene oxide *Compos. Sci. Technol.* **186** 107912
- [25] Chen Y, Lin B, Zhang X, Wang J, Lai C, Sun Y, Liu Y and Yang H 2014 Enhanced dielectric properties of amino-modified-CNT/polyimide composite films with a sandwich structure *J. Mater. Chem. A* **2** 14118–26
- [26] Feng Y F, Zhou F R, Dai Y M, Xu Z C, Deng Q H and Peng C 2020 High dielectric and breakdown performances achieved in PVDF/graphene@MXene nanocomposites based on quantum confinement strategy *Ceram. Int.* **46** 17992–8001
- [27] Hu J, Zhang S and Tang B 2021 2D filler-reinforced polymer nanocomposite dielectrics for high-k dielectric and energy storage applications *Energy Storage Mater.* **34** 260–81
- [28] Kadir E S, Gayen R N, Paul R and Biswas S 2020 Interfacial effects on ferroelectric and dielectric properties of GO reinforced free-standing and flexible PVDF/ZnO composite membranes: bias dependent impedance spectroscopy *J. Alloys Compd.* **843** 11
- [29] Kumar M et al 2016 Preparation and characterization of low fouling novel hybrid ultrafiltration membranes based on the blends of G0-TiO₂ nanocomposites and polysulfone for humic acid removal *Journal of Membrane Science* **506** 38–49
- [30] Dang Z M, Zheng M S and Zha J W 2016 1D/2D carbon nanomaterial-polymer dielectric composites with high permittivity for power energy storage applications *Small* **12** 1688–701
- [31] Huang X Y, Sun B, Zhu Y K, Li S T and Jiang P K 2019 High-k polymer nanocomposites with 1D filler for dielectric and energy storage applications *Prog. Mater. Sci.* **100** 187–225
- [32] Zhang H, Marwat M A, Xie B, Ashtar M, Liu K, Zhu Y, Zhang L, Fan P, Samart C and Ye Z G 2020 Polymer matrix nanocomposites with 1D ceramic nanofillers for energy storage capacitor applications *ACS Appl. Mater. Interfaces* **12** 1–37
- [33] Bao Z et al 2020 Negatively charged nanosheets significantly enhance the energy-storage capability of polymer-based nanocomposites *Adv. Mater.* **32** 1907227
- [34] Chen J, Wang Y, Dong J, Chen W and Wang H 2021 Ultrahigh energy storage density at low operating field strength achieved in multicomponent polymer dielectrics with hierarchical structure *Compos. Sci. Technol.* **201** 108557
- [35] Feng M J, Zhang T D, Song C H, Zhang C H, Zhang Y, Feng Y, Chi Q G, Chen Q G and Lei Q Q 2020 Improved energy storage performance of all-organic composite dielectric via constructing sandwich structure *Polymers* **12** 1972
- [36] Huang C, Zhang L, Liu S, Wang Y, Wang N and Deng Y 2021 Double enhanced energy storage density via polarization

- gradient design in ferroelectric poly(vinylidene fluoride)-based nanocomposites *Chem. Eng. J.* **411** 128585
- [37] Li Q, Liu F, Yang T, Gadinski M R, Zhang G, Chen L-Q and Wang Q 2016 Sandwich-structured polymer nanocomposites with high energy density and great charge-discharge efficiency at elevated temperatures *Proc. Natl Acad. Sci.* **113** 9995–10000
- [38] Liang X W, Yu X C, Lv L L, Zhao T, Luo S B, Yu S H, Sun R, Wong C P and Zhu P L 2020 BaTiO₃ internally decorated hollow porous carbon hybrids as fillers enhancing dielectric and energy storage performance of sandwich-structured polymer composite *Nano Energy* **68** 104351
- [39] Lin Y, Sun C, Zhan S L, Zhang Y J, Yang H B and Yuan Q B 2020 Two-dimensional sheet-like K_{0.5}Na_{0.5}NbO₃ platelets and sandwich structure induced ultrahigh discharge efficiency in poly (vinylidene fluoride)-based composites *Compos. Sci. Technol.* **199** 108368
- [40] Lin Y, Zhang Y J, Zhan S L, Sun C, Hu G L, Yang H B and Yuan Q B 2020 Synergistically ultrahigh energy storage density and efficiency in designed sandwich-structured poly (vinylidene fluoride)-based flexible composite films induced by doping Na_{0.5}Bi_{0.5}TiO₃ whiskers *J. Mater. Chem. A* **8** 23427–35
- [41] Liu Y, Hou Y F, Ji Q, Wei S X, Du P, Luo L H and Li W P 2020 Modulation of individual-layer properties results in excellent discharged energy density of sandwich-structured composite films *J. Mater. Sci., Mater. Electron.* **31** 7663–71
- [42] Marwat M A, Ma W G, Fan P Y, Elahi H, Samart C, Nan B, Tan H, Salamon D, Ye B H and Zhang H B 2020 Ultrahigh energy density and thermal stability in sandwich-structured nanocomposites with dopamine@Ag@BaTiO₃ *Energy Storage Mater.* **31** 492–504
- [43] Marwat M A, Xie B, Zhu Y W, Fan P Y, Liu K, Shen M, Ashtar M, Kongparakul S, Samart C and Zhang H B 2019 Sandwich structure-assisted significantly improved discharge energy density in linear polymer nanocomposites with high thermal stability *Colloid Surf. A* **581** 123802
- [44] Marwat M A et al 2019 Largely enhanced discharge energy density in linear polymer nanocomposites by designing a sandwich structure *Composites A* **121** 115–22
- [45] Marwat M A, Yasar M, Ma W G, Fan P Y, Liu K, Lu D J, Tian Y, Samart C, Ye B H and Zhang H B 2020 Significant energy density of discharge and charge-discharge efficiency in Ag@BNN nanofillers-modified heterogeneous sandwich structure nanocomposites *Acs Appl. Energ. Mater.* **3** 6591–601
- [46] Sun Q Z, Mao P, Zhang L X, Wang J P, Zhao Y Y and Kang F 2020 Significantly enhanced dielectric and energy storage performance of AlN/KNbO₃/PVDF sandwich-structured composites via introducing the AlN/PVDF insulating layers *Ceram. Int.* **46** 9990–6
- [47] Wang Y, Wang L, Yuan Q, Niu Y, Chen J, Wang Q and Wang H 2017 Ultrahigh electric displacement and energy density in gradient layer-structured BaTiO₃/PVDF nanocomposites with an interfacial barrier effect *J. Mater. Chem. A* **5** 10849–55
- [48] Wang Y F, Cui J, Yuan Q B, Niu Y J, Bai Y Y and Wang H 2015 Significantly enhanced breakdown strength and energy density in sandwich-structured barium titanate/poly (vinylidene fluoride) nanocomposites *Adv. Mater.* **27** 6658–63
- [49] Zhang Y, Zhang T, Liu L, Chi Q, Zhang C, Chen Q, Cui Y, Wang X and Lei Q 2018 Sandwich-structured PVDF-based composite incorporated with hybrid Fe₃O₄@BN nanosheets for excellent dielectric properties and energy storage performance *J. Phys. Chem. C* **122** 1500–12
- [50] Chen J, Yao B, Li C and Shi G 2013 An improved Hummers method for eco-friendly synthesis of graphene oxide *Carbon* **64** 225–9
- [51] Zhang T, Guo M, Jiang J, Zhang X, Lin Y, Nan C-W and Shen Y 2019 Modulating interfacial charge distribution and compatibility boosts high energy density and discharge efficiency of polymer nanocomposites *RSC Adv.* **9** 35990–7
- [52] Guan L, Weng L, Zhang X, Wu Z, Li Q and Liu L 2020 Microstructures, electrical behavior and energy storage properties of Ag@shell/PVDF-based polymers: different effects between an organic polydopamine shell and inorganic zinc oxide shell *J. Mater. Sci.* **55** 15238–51
- [53] Liu S and Zhai J 2015 Improving the dielectric constant and energy density of poly(vinylidene fluoride) composites induced by surface-modified SrTiO₃ nanofibers by polyvinylpyrrolidone *J. Mater. Chem. A* **3** 1511–7
- [54] Wang S, Huang X, Wang G, Wang Y, He J and Jiang P 2015 Increasing the energy efficiency and breakdown strength of high-energy-density polymer nanocomposites by engineering the Ba_{0.7}Sr_{0.3}TiO₃ nanowire surface via reversible addition–fragmentation chain transfer polymerization *J. Phys. Chem. C* **119** 25307–18
- [55] Wu L, Wu K, Liu D, Huang R, Huo J, Chen F and Fu Q 2018 Largely enhanced energy storage density of poly(vinylidene fluoride) nanocomposites based on surface hydroxylation of boron nitride nanosheets *J. Mater. Chem. A* **6** 7573–84
- [56] Yao L, Pan Z, Zhai J, Zhang G, Liu Z and Liu Y 2018 High-energy-density with polymer nanocomposites containing of SrTiO₃ nanofibers for capacitor application *Composites A* **109** 48–54